Tidal exchange through the Kuril Straits

Toshiyuki AWAJI[1], Tomohiro Nakamura[1], Takaki Hatayama[1], Kazunori Akitomo[1] and Takatoshi Takizawa[2]

[1] Department of Geophysics, Kyoto University, Kyoto, Japan

[2] Japan Marine Science and Technology Center, Yokosuka, Japan

Abstract. The tidal exchange between the Okhotsk Sea and the North Pacific Ocean is studied numerically with particular emphasis on the predominant component, the barotropic K_1 tide. Since the K_1 tide is subinertial in the Okhotsk Sea, topographically trapped waves are effectively generated, contributing to strong tidal currents with a maximum amplitude of over 1.5 m s^{-1} in the Kuril Straits. The structures of tide-induced mean flows in most passages of the Straits are characterized by "bi-directional currents" (in which the mean flow exhibits a reversal in direction across the passages). The mean transport shows significant net exchange of water via several straits in the Kuril Islands, whose amount is over 5.0 Sv toward the North Pacific. Therefore, the tidal current is thought to play a major role in water exchange processes between the Okhotsk Sea and the North Pacific. Our analysis reveals that the bi-directional mean currents at shallow passages are produced through the well known process of tidal rectification, whereas in deep passages, the propagating trapped waves along islands are essential for generating the bi-directional mean currents.

Introduction

The Okhotsk Sea (Fig. 1) is thought to have a significant impact upon the North Pacific. For example, Talley (1993) and Yasuda et al. (1996) commented that the Okhotsk Sea supplies low salinity water to the North Pacific Intermediate Water (NPIW) characterized by a salinity minimum centered at $26.8\sigma_\theta$. Thus, a clarification of the exchange processes through the Kuril Straits is indispensable for a better understanding of water mass formation in the North Pacific (such as the NPIW). Past studies regarded the current in the Okhotsk Sea as part of the cyclonic subarctic circulation which predominantly flows into the Okhotsk Sea through the Kruzenshtern Strait and out through the Bussol Strait. However, recent observational studies suggest that there is great difficulty in explaining this in/outflow in terms of geostrophic balance. One reason for this is that the overall surface dynamic height is higher in the Okhotsk Sea than in the northwestern North Pacific (Kawasaki and Kono, 1992). Another reason is that due to the weak stratification, the Oyashio extends to such depths that it tends to flow along the continental shelf slope along the Kuril Islands (2000 $\sim$ 3000 m deep) and is plausibly unable to pass over the shallow sills in the Kuril Straits. Moreover, Leonov (1960) and Moroshkin (1966) mentioned that bi-directional currents occur in most passages. This picture is clearly seen in the NOAA 12 AVHRR imagery (not shown). Such current structures cannot be explained by large-scale wind-driven geostrophic flow. These observational results strongly suggest the importance of non-geostrophic components. In fact, tidal currents, especially diurnals, are dominant in and around the Kuril Straits, and their speeds reach a few knots. According to previous studies on tidal exchange (Awaji et al., 1980), such strong tidal currents are expected to induce significant mean transport, even if there are sills in the straits. Moreover, tide-induced mean currents allow us to explain the bi-directional structure of the (local) mean currents in the passages. Thus, as a first step toward understanding the transport process, we have investigated numerically the characteristics of the tides and tidal currents around the Okhotsk Sea.

Model

The model region (Fig. 1) covers the entire Okhotsk Sea and part of the North Pacific. The open boundaries are set away from the Okhotsk Sea in order to reproduce tidal wave propagation from the North Pacific. We resolved the topography of the model region using 5 km $\times$ 5 km grids. The numerical model is the same as that used by Hatayama et al. (1996) with the familiar barotropic global tidal equations (e.g., Schwiderski, 1979a). The boundary conditions are set as follows. A no-slip condition is imposed at the land boundaries. At the open boundaries, the tidal elevation for K_1 and M_2 is specified

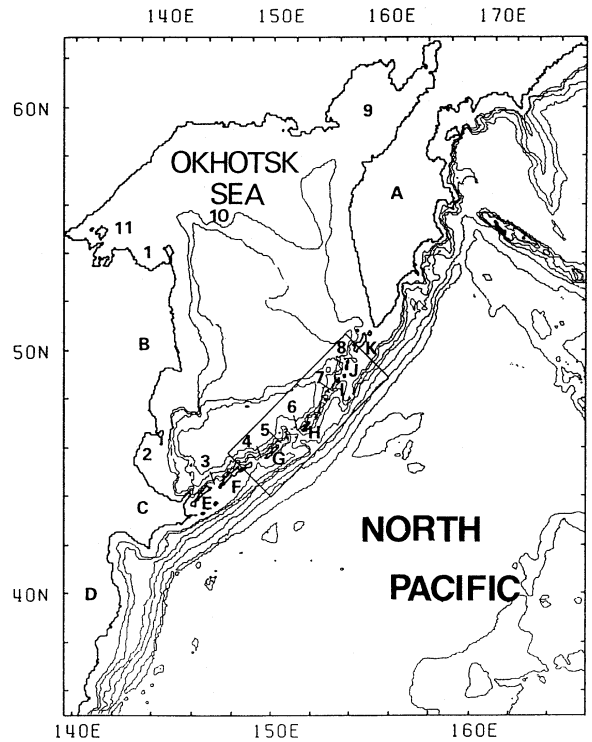

Fig. 1 Model domain and topography. Main straits of the Kuril (3–8, E–K) are the Bussol (6), Kruzenshtern (7), Chetvertyy (8) Straits. The Kashevarov Bank and Kamchatka Peninsula are indicated by 10 and A, respectively.

separately using previous results (e.g., Schwiderski, 1979a,b). Thus, the model is forced by these boundary oscillations in addition to the effects of the tide generating potential, the Earth tide, and the ocean loading tide. We performed 24 cycles of the integration, by which time the model ocean reached an almost steady oscillation and the final cycle of simulation is used for the analysis described below.

Tidal fields in the Okhotsk Sea

The harmonic constants (sea-level amplitude and phase) are calculated at every grid point, and the spatial distributions of the co-amplitude and co-phase lines obtained for K_1 and M_2 tides (not shown) are qualitatively consistent with previous studies (Mazzega and Bérge, 1994), respectively. To check the calculated fields quantitatively, we made a comparison with the International Hydrographic Office (IHO) tidal harmonic constants. For the predominant component K_1 tide, the correlation coefficients between the calculated and the observed harmonic constants are high (0.904 for phase and 0.976 for amplitude). For the M_2 tide, the correlation coefficients are also high (0.825 for amplitude and 0.929 for phase). Thus it can be said that the calculated tidal fields have good similarities compared to those observed and the current fields are expected to be fairly reliable. To study the features of the tidal currents in the Okhotsk Sea, we calculated the ellipse parameters shown in Figure 2. The K_1 tide has the greatest current speed. The currents are strong and their tidal ellipses are circular around topographic features, such as the Kuril Straits and the Kashevarov Bank. For example, the peak velocity in the northern part of the Kuril Straits reaches about 1.6 m s^{-1}. These features are associated with the fact that the period of the K_1 tide is longer than the inertial period around the Kuril Straits. Since subinertial tidal currents generate subinertial waves trapped at islands and/or submarine banks, the topographically trapped waves are subjected to continuous forcing and are enhanced until damping by friction or viscosity becomes important. The resulting amplification of trapped waves is most effective when the resonance occurs but is significant for a wide range if the tidal frequency is subinertial. Therefore the K_1 tide is expected to cause significant tide-induced mean flow around the Straits. On the other hand, the M_2 tide is significantly smaller in current speed than the K_1 tide, despite the fact that their elevation amplitudes are comparable. In fact, the maximum value around the Kuril Straits is only 0.6 m s^{-1}. The tidal ellipses are not circular around the Kuril Straits. Since the M_2 tide is superinertial, amplification hardly occurs and the currents are weak in the Kuril Straits, indicating that the mean currents induced by the M_2 tide are probably not significant.

Eulerian mean currents and estimates of tidal exchange through the Kuril Straits

Based on the depth-averaged velocity vectors of the Eulerian time-averaged currents over a cycle, we calculated the stream function of the mean volume transport ψ, which is defined as

$$(\overline{u}, \overline{v}) = \left(-\frac{1}{H}\frac{\partial \psi}{\partial y}, \ \frac{1}{H}\frac{\partial \psi}{\partial x} \right) \qquad (1)$$

with the zero point taken at the Kamchatka Peninsula. The result for the K_1 tide is shown in Figure 3. In general, the mean currents are almost parallel to the isobaths and form clockwise mean currents around the islands, leading to bi-directional mean currents in most passages and strong clockwise along-sill (or along-island) mean currents. Tak-

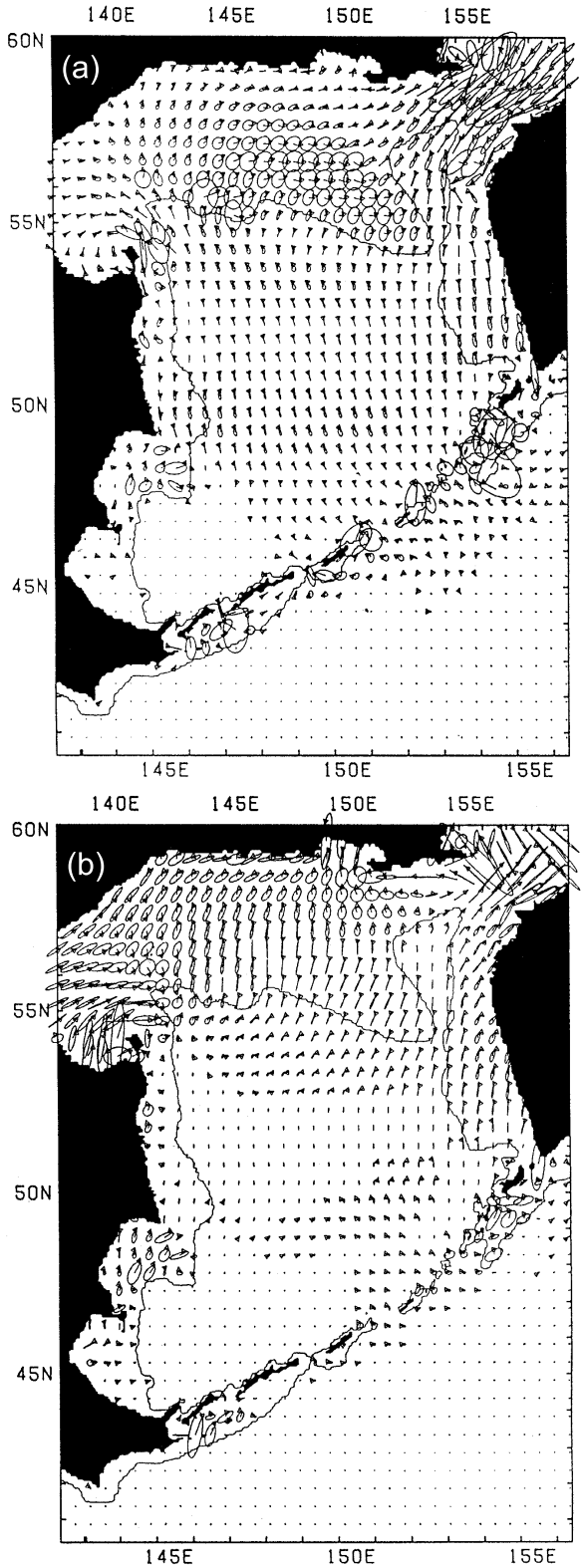

Fig. 2 Calculated tidal ellipses for (a) the K_1 tide and (b) the M_2 tide. The magnitude of velocity for (a) is 15 cm s^{-1} and for (b) is 30 cm s^{-1}.

ing the bi-directional currents into account, we estimated the total transport for all the straits with this mean current field. For K_1 (Fig. 4), most of the exchange occurs at the Bussol Strait and the northeastern part of the Kuril Straits. In terms of magnitude, the net transport of about 5.0 Sv from the Okhotsk Sea to the North Pacific occurs mainly through the Bussol (2.4 Sv), Kruzenshtern (0.8 Sv) and Chetvertyy (0.8 Sv) Straits. Inflow transport is largest (1.45 Sv) through the Bussol Strait followed by 1.2 Sv through the Kruzenshterna Strait. When neglecting the bi-directional flow, the total transport comes to 2.2 Sv, indicating that current meter deployment capable of resolving the bi-directional current structure is required to estimate the total transport observationally. Transport estimates made with the O_1, P_1, M_2, and S_2 tides are 3.5, 1.0, 0.3, and 0.1 Sv, respectively, showing that transport induced by diurnal tides is much greater than that by semidiurnal tides.

Formation mechanism of bi-directional mean currents

Figure 5 shows the Eulerian mean relative vorticity over a cycle around the Kuril Straits. According to previous studies of tidal rectification (Robinson, 1981), the mean vorticity generally acquires negative values on the sill top and positive values at the base

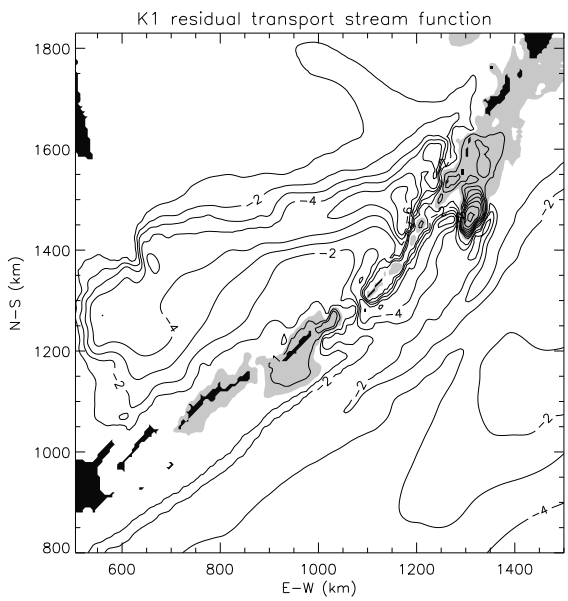

Fig. 3 Mean transport stream function for the K_1 tide, which is set to be zero at the Kamchatka Peninsula. The contour units are 0.4 Sv and values in shaded areas are positive.

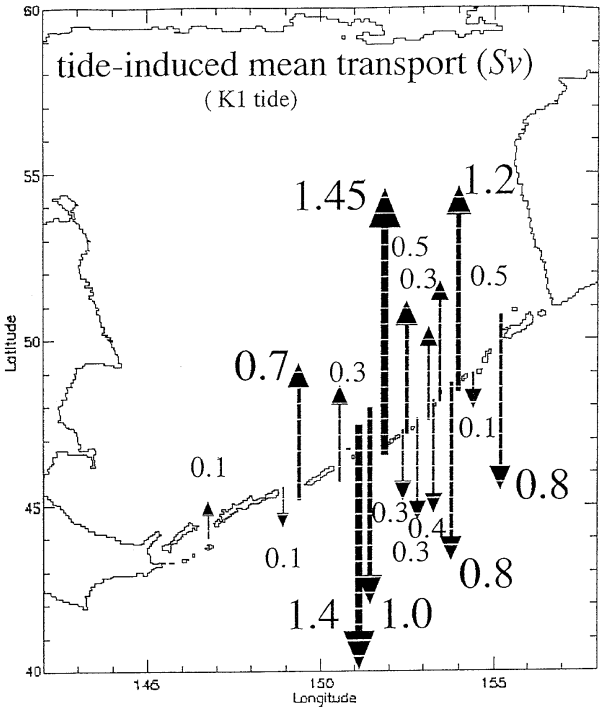

Fig. 4 The estimate of the mean transport through the Kuril Straits induced by the K_1 tide. Upward and downward arrows represent inflow and outflow, respectively.

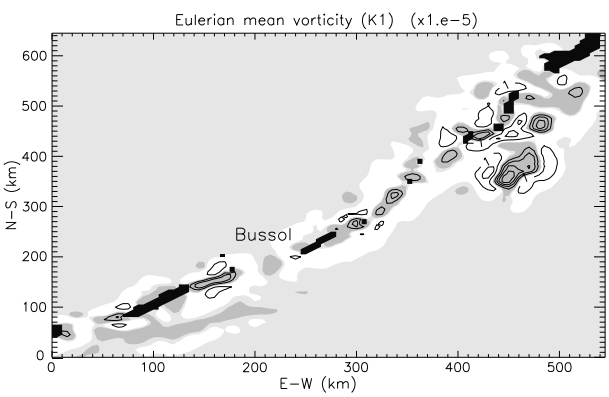

Fig. 5 The Eulerian mean relative vorticity over one cycle around the Kuril Straits for the K_1 tide. The contour interval is 1×10^{-5} s^{-1}. Values in unshaded areas and the dark shaded areas are positive and negative, respectively, and the absolute values in the light shaded areas are less than 1×10^{-6} s^{-1}.

of the sill, which, in turn, produce a clockwise mean current along the sill. Such a pattern is clearly seen in shallow straits (200 ~ 600 m depth), and as the sill gets higher in the vicinity of the islands, the magnitude of the negative mean vorticity on top of the sill becomes larger. Supposing mass conservation of the along-sill mean currents, such vorticity changes in shallow straits lead to clockwise mean circulation on island scales, thus creating bi-directional mean currents in shallow straits as shown schematically in Figure 6. In deep straits, on the other hand, the mean vorticity distribution on the sill top has positive values near the islands. This vorticity pattern differs greatly from that in shallow straits in spite of the presence of similar bi-directional currents. To investigate this problem, we direct our attention to the Bussol Strait, where the sill is very deep, bi-directional currents are dominant, and hence most of the outflow from the Okhotsk Sea occurs.

To examine the cause for the different vorticity distribution between deep and shallow straits, we diagnose the vorticity balance in a similar way to Ridderinkhof (1989). The result shows that, as in past studies, the stretching/squeezing effects are basically dominant in vorticity generation. These fea-

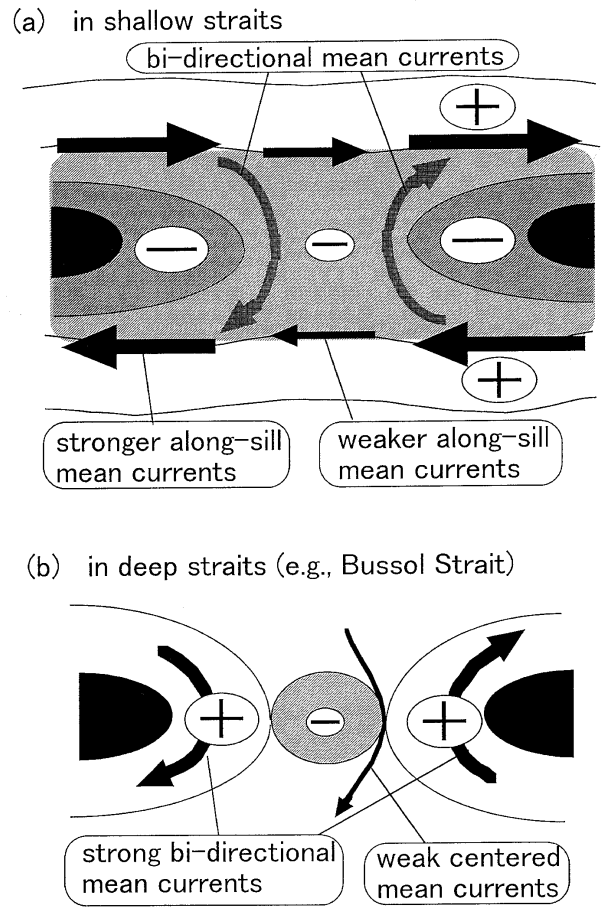

Fig. 6 Schematic illustrations of mean currents associated with the mean vorticity distribution in (a) shallow straits (200 ~ 600 m depth) and (b) deep straits (the case of the Bussol Strait).

tures are present at most straits. Thus, the vorticity balance for generating bi-directional mean currents is the same in both shallow and deep straits, despite the fact that their vorticity distribution differs mutually. This implies the presence of a different mechanism from the previous tidal rectification theory for the formation of the mean circulation in deep straits. The most likely candidate for this is the effect of topographically trapped waves, because it is anticipated that for subinertial tides the transport of vorticity anomaly by the waves becomes effective in the vorticity balance. Detailed analysis using the vorticity equation revealed that the transport of vorticity anomaly around the Kuril Islands is basically determined by the following equation:

$$\left(\frac{\partial}{\partial t} + (\boldsymbol{u}_{across} + \boldsymbol{u}_{along} + \boldsymbol{c}) \cdot \nabla\right) \omega_{wave} + \left(\frac{\partial}{\partial t} + \boldsymbol{u} \cdot \nabla\right)(\omega - \omega_{wave}) = -\frac{f}{H} \nabla H \cdot \boldsymbol{u}^{irr}_{across} + \text{ damping }, \qquad (2)$$

where $\boldsymbol{c} = (c_x, c_y)$ is the phase velocity of a nondivergent linear topographic Rossby wave given as

$$c_x = \frac{H_y}{k^2 + l^2} \frac{f}{H}, \qquad c_y = -\frac{H_x}{k^2 + l^2} \frac{f}{H}. \qquad (3)$$

The term ω_{wave} is the vorticity associated with the wave component. This equation shows that the vorticity component $(\omega - \omega_{wave})$ is transported only by tidal currents and causes the well known process of tidal rectification. On the other hand, the vorticity anomaly ω_{wave} is transported not only by the currents $(\boldsymbol{u}_{across} + \boldsymbol{u}_{along})$ but also by topographically trapped waves propagating with a phase velocity $\boldsymbol{c}$ (thus, there are additional vorticity changes caused by the propagation of topographically trapped waves at any location along the island chain). Accordingly, topographically trapped waves are able to affect the mean field at locations well away from the generation region of vorticity. In the northern hemisphere, the phase velocity $\boldsymbol{c}$ of topographically trapped waves is in the along-isobath direction with shallower regions on the right. The along-sill (along-isobath) current flows with positive and negative values of vorticity to their left and right, respectively (not shown). On the positive vorticity side of the sill, the along-sill current is in the same direction as the phase velocity $\boldsymbol{c}$ of the topographically trapped waves of positive vorticity. In contrast, on the negative vorticity side of the sill, the along-sill current is in the opposite direction to the propagation of topographic waves of negative vorticity. Consequently, the topographically trapped waves of positive vorticity move faster than those of negative vorticity. This means that the magnitude of the positive vorticity flux created by topographically trapped waves in the along-isobath direction is larger than that of the negative vorticity flux over a tidal cycle, and eventually leads to the presence of a net flux of positive vorticity in a clockwise sense around the islands. In shallow straits, since topographically trapped waves hardly cross the shallow sills, this process has little effect on the formation of mean vorticity. In contrast, in deep and wide straits such as the Bussol and Kruzenstern Straits, mean vorticity generation through the tidal rectification process is small but the topographically trapped waves coming from shallow straits can cross the deep sills, thus producing positive mean vorticity. This leads to the formation of the bi-directional mean current structures around both ends of the deep sills.

Summary and discussion

Our regional model has shown that the Eulerian mean outflow from the Okhotsk Sea can reach the significant value of 5.0 Sv for the K_1 tide, the main part of which is conducted through the Bussol, Kruzenshtern, and Chetvertyy Straits. This significant tidal exchange is produced by bi-directional mean currents in the Straits, which are consistent with the current structure observed in infrared images taken by NOAA 12 and mentioned in earlier work by Moroshkin (1966) and Leonov (1960). Therefore, it is suggested that tidal currents play an important role in water exchange between the Okhotsk Sea and the North Pacific, although precise quantitative discussions will await future observations. We showed that the mean currents are produced through the effects of topographically trapped waves as well as through well known tidal rectification. In shallow straits (200 $\sim$ 600 m depth), tidal rectification mainly due to advection, vorticity generation by the stretching/squeezing effect, and damping by bottom friction produces the strong along-sill and weak bi-directional mean currents. On the other hand, in deep straits such as the Bussol Strait, a net flux of positive vorticity from the adjacent shallow straits to the deep strait is caused by topographically trapped waves and produces strong bi-directional mean currents there. This net flux is caused by the fact that the along-isobath currents are in the same direction as the phase velocity of the topographically trapped waves with positive vorticity, and are in the opposite direction to that with negative vorticity. We have clarified the outline of the horizontal exchange induced by the tidal currents.

However, since we use a two-dimensional barotropic model, the vertical structure is still unclear. Therefore, an investigation of the vertical structure of tidal currents around the Straits, which includes the baroclinic effect, may be important for our understanding of the detailed transport processes as well as the effect of wind-driven large-scale geostrophic flow and eddies on water exchange and mixing around the Kuril Straits.

References

Awaji, T., Imasato, N. and Kunishi, K. 1980. Tidal exchange through a strait: A numerical experiment using a simple model basin. *J. Phys. Oceanogr., 10*, 1499–1508.

Hatayama, T., Awaji, T. and Akitomo, K. 1996. Tidal currents in the Indonesian Seas and their effect on transport and mixing. *J. Geophys. Res., 101*, 12,353–12,373.

Kawasaki, Y. and Kono, T. 1992. Baroclinic water exchange in the Kuril Basin and the northwestern Pacific in summer. *Sea and Sky, 68*, 41–54. (in Japanese)

Leonov, A.K. 1960. *Regional Oceanography. Part 1.* Gidrometeoizdat, Leningrad, pp. 226–229.

Mazzega, P. and Bergé, M. 1994. Ocean tides in the Asian semienclosed seas from TOPEX/POSEIDON. *J. Geophys. Res., 99*, 24,867–24,881.

Moroshkin, K.V. 1966. Water masses of the Sea of Okhotsk. U.S. Department of Commerce, Clearing-house for Federal Scientific and Technical Information, Joint Publication Research Service, *43*, 942. 98 pp.

Ridderinkhof, H. 1989. Tidal and residual flows in the Western Dutch Wadden Sea: Vorticity balances. *Neth. J. Sea Res., 24*, 9–16.

Robinson, I.S. 1981. Tidal vorticity and residual circulation, *Deep-Sea Res., 28a*, 195–212.

Schwiderski, E.W. 1979a. Global Ocean Tides, II: The semidiurnal principal lunar tide (M_2). In *Atlas of Tidal Charts and Maps, Naval Surface Weapons Center NSWC-TR.*

Schwiderski, E.W., 1979b. Global Ocean Tides, IV: The diurnal luni-solar declination tide (K_1). In *Atlas of Tidal Charts and Maps, Naval Surface Weapons Center NSWC-TR.*

Talley, L.D. 1993. Distribution and formation of North Pacific Intermediate Water. *J. Phys. Oceanogr., 23*, 517–537.

Yasuda, I., Okuda, K. and Shimizu, Y. 1996. Distribution and formation of North Pacific Intermediate Water in the Kuroshio-Oyashio interfrontal zone. *J. Phys. Oceanogr., 26*, 448–465.